In situ differential reflectance spectroscopy of thin crystalline films of PTCDA on different substrates

Holger Proehl, Robert Nitsche, Thomas Dienel, Karl Leo, and Torsten Fritz*
Institut für Angewandte Photophysik, Technische Universität Dresden, D-01062 Dresden, Germany
(Received 15 September 2004; published 22 April 2005)

We report an investigation of the excitonic properties of thin crystalline films of the archetypal organic semiconductor PTCDA (3,4,9,10-perylenetetracarboxylic dianhydride) grown on poly- and single crystalline surfaces. A sensitive setup capable of measuring the optical properties of ultrathin organic molecular crystals via differential reflectance spectroscopy (DRS) is presented. This tool allows to carry out measurements *in situ*, i.e., during the actual film growth, and over a wide spectral range, even on single crystalline surfaces with high symmetry or metallic surfaces, where widely used techniques like reflection anisotropy spectroscopy (RAS) or fluorescence excitation spectroscopy fail. The spectra obtained by DRS resemble mainly the absorption of the films if transparent substrates are used, which simplifies the analysis. In the case of mono- to multilayer films of PTCDA on single crystalline muscovite mica(0001) and Au(111) substrates, the formation of the solid state absorption from monomer to dimer and further to crystal-like absorption spectra can be monitored.

DOI: 10.1103/PhysRevB.71.165207 PACS number(s): 78.20.−e, 78.66.Qn, 78.40.Me, 81.15.Hi

I. INTRODUCTION

Organic semiconductors have recently attracted increasing interest, mainly due to potential optoelectronic applications like organic electroluminescence displays and organic solar cells.[1,2] A considerable advantage, besides their low production costs, is the large variety of potential compounds which can be synthesized by organic chemistry. Highly ordered thin molecular films, ultrathin organic molecular crystals (OMC), as can be prepared by organic molecular beam epitaxy (OMBE), can provide a deeper insight into the physical processes occurring in organic devices, because the optical and electronic properties of organic molecular single crystals depend very sensitively on the intermolecular interactions within the crystal. The molecule 3,4,9,10-perylenetetracarboxylic dianhydride (PTCDA) represents an archetype for organic thin film growth. It usually forms smooth and highly ordered layers on a large variety of different substrates.[1,3–7] The structural and optical properties of perylene derivative thin films on different substrate surfaces have been studied in detail. The confinement of delocalized excitons was proposed to explain findings like a blueshift of absorption or fluorescence with decreasing film thickness, although other explanations were proposed in several publications.[8–12] Much effort has been put into the understanding of the absorption spectra of both the PTCDA crystal and vacuum deposited thin films.[13–16] To prove these theories, high precision measurements of the optical properties are required. Recently it was pointed out that the monomer-dimer-oligomer transition is an essential key to understand the optical properties of the quasi-one-dimensional molecular crystal of PTCDA.[17]

Here, we want to give a more comprehensive discussion of the findings for PTCDA grown on muscovite mica(0001), explained rather briefly in Ref. 17, as well as a comparison with the case of PTCDA on Au(111). We will show that an optical *in situ* characterization of thin films by the method of differential reflectance spectroscopy (DRS) not only provides a high precision, but also permits the exclusion of effects like reorganization of the film occurring at measurements in ambient conditions.

This paper is divided into two parts: We first describe the principle of the DRS measurement and *in situ* setup, second, we report on a comparative optical investigation by DRS as well as optical density measurements of ultrathin PTCDA films on different kinds of substrates; to demonstrate the rather universal potential of the method and of our setup.

II. MEASUREMENT PRINCIPLE

In organic-inorganic heteroepitaxy, conductive and opaque substrates, e.g., metallic single crystals, are often used to allow the use of structural characterization methods like scanning tunnelling microscopy (STM) and low-energy electron diffraction (LEED). Therefore, only the reflectance of the sample is accessible by optical investigation. To distinguish between the properties of the adsorbate film and those of the substrate, differential methods are required. Several approaches are conceivable: (i) the difference in reflectance under different polarization angles will lead to reflectance anisotropy spectroscopy (RAS), (ii) comparison of the reflectance of the bare and the adsorbate-covered sample is the basis for (surface) differential reflectance spectroscopy (SDRS/DRS), being our method of choice.

DRS serves as a powerful method to investigate ultrathin films or adsorbed species and can be applied not only in surface physics, but also in physical chemistry and electrochemistry, e.g., for monitoring processes on electrodes in electrolyte solutions. There are detailed reviews about the latter applications in literature.[18–20] In a DRS measurement, the respective intensities of the reflected light from the adsorbate covered and the bare sample, $R(\omega)$ and $R_0(\omega)$, are compared,

$$\frac{\Delta R}{R}(\omega) = \frac{R(\omega) - R_0(\omega)}{R_0(\omega)}. \quad (1)$$

The $\Delta R/R$ signal is composed of the signal of the underlying substrate perturbed by the presence of an absorbing adsor-

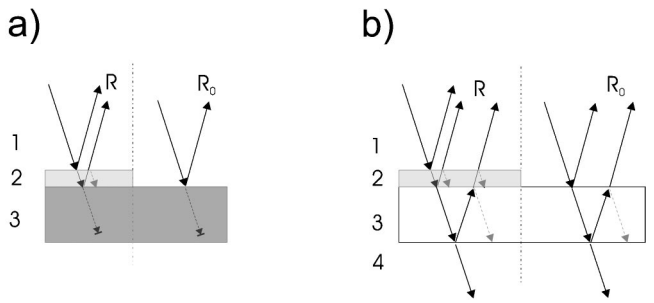

FIG. 1. Reflectance of the adsorbate covered and bare sample in case of (a) an opaque substrate and (b) a transparent substrate.

bate film on top of it, as can be seen in Fig. 1. The dependency of the signal on the angle of incidence and on the optical constants of substrate and film are given by the Fresnel equations. For very thin films of atoms or molecules exhibiting thicknesses much smaller than the wavelength of light, the Fresnel equations of the two-interface system (ambient-adsorbate film-substrate) can be linearized. For opaque or semi-infinite substrates at normal incidence of light (nearly fulfilled here) and vacuum ($\epsilon_1=1$), the linearization results in a comparatively simple expression:[21]

$$\frac{\Delta R}{R} \cong -\frac{8\pi d_2}{\lambda}\mathrm{Im}\left(\frac{1-\hat{\epsilon}_2}{1-\hat{\epsilon}_3}\right), \tag{2}$$

where d_2 is the thickness and $\hat{\epsilon}_2$ the (complex) dielectric function (DF) of the molecular layer.[22] Consequently, the DRS signal $\Delta R/R$ consists of a mixture (of the imaginary and real parts) of the dielectric functions of the substrate $\hat{\epsilon}_3$ and adsorbate $\hat{\epsilon}_2$.

For highly transparent substrates like mica, there is only weak absorption in the wavelength range of interest. The imaginary part of $\hat{\epsilon}_3$ is very small, and hence Eq. (2) can be further simplified to $[\mathrm{Im}(\hat{\epsilon}_3)\ll 1, \mathrm{Re}(\hat{\epsilon}_3)=\epsilon_3]$

$$\frac{\Delta R}{R} \cong \frac{8\pi d_2}{\lambda}\frac{\mathrm{Im}(\hat{\epsilon}_2)}{1-\epsilon_3}. \tag{3}$$

In the case of mica, where ϵ_3 is almost constant over the visible wavelength range, the DRS signal mainly represents the imaginary part of the dielectric function of the adsorbate film (compare Fig. 2). However, in most experiments the substrate will be rather thin, and the backside reflection of the substrate has to be taken into account [Fig. 1(b)]. A linearization of the Fresnel expression of the resulting three-interface system for very thin coherent adsorbate layers on an incoherent substrate leads to a practical expression only in case of normal incidence

$$\frac{\Delta R}{R}(\hat{\epsilon}_2,\hat{\epsilon}_3,d_2,d_3) \cong \frac{\Delta R}{R}(\hat{\epsilon}_2,\hat{\epsilon}_3,d_2)|_{d_3=\infty} F(\hat{n}_3,d_3). \tag{4}$$

In the limit of an nearly transparent substrate ($\mathrm{Im}[\hat{\epsilon}_3]\rightarrow 0, \mathrm{Re}[\hat{\epsilon}_3]\approx\epsilon_3=n_3^2$), the function F is almost aspectral and can be expressed by a Taylor series in zero or first order in d_3, while the first part of Eq. (4) is treated analogously to Eq. (3) Practically, one would estimate F by a comparison of the full Fresnel expressions for $\Delta R/R$ in case of a finite and an

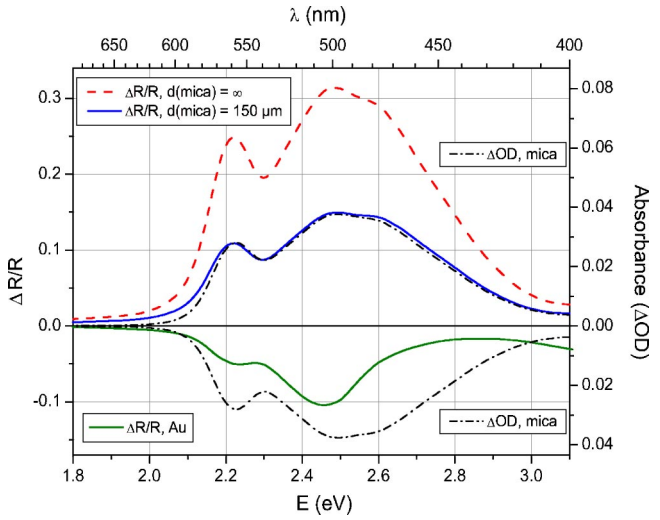

FIG. 2. (Color online) Simulated DRS of a 2 nm polycrystalline PTCDA film on Au (lower part), on a semi-infinite mica substrate, and a mica sample of a typical thickness used (150 μm) (upper part) in comparison with the absorbance spectra (differential Optical Density, ΔOD) of that film [optical constants of polycrystalline PTCDA from Ref. 27]. Note the similarity between $\Delta R/R$ and ΔOD in case of the substrate mica: only a small shift of the low energy peak at 2.22 eV of ~8 meV occurs.

infinite substrate for a correspondingly chosen value of $\hat{\epsilon}_3$. For the mica sheets (thickness of 100–190 μm) used here and a refractive index of about $n_3=1.6$ in the visible spectral range, this will cause a lowering of the DRS signal by a factor of about $F\approx 0.5$.

While all the approximate equations given above and below are useful to understand the principal dependence of the measured DRS signal on the optical constants and film thicknesses involved, all further simulations of DR spectra are done by using the full set of Fresnel equations, for the most part with commercial thin film optics software.[23] When doing so, we found that it is not necessary to consider the exact experimental geometry at 20° angle of incidence (discrimination between p, s polarization): the influence of the deviation of the angle of incidence from 0° on the DRS signal is less than 1.5% for the entire absorption range of PTCDA for both the gold and mica substrate, if nonpolarized light is used.

In Fig. 2, it can be seen that in case of transparent substrates, the DRS signal represents nearly the absorbance [i.e., the differential optical density (ΔOD), given by the difference of the absorbance of the sample before and after film deposition] of the thin adsorbate film. A linearization of the corresponding Fresnel equations for the case of ultrathin films yields for the differential optical density ΔOD of the adsorbate film, an equation directly proportional to $\mathrm{Im}(\hat{\epsilon}_2)$ (transparent incoherent thick substrate)[24]

$$\Delta\mathrm{OD} \cong \frac{1}{\ln(10)}\frac{\Delta T}{T} \cong \frac{4\pi d_2}{\lambda\ln(10)}\frac{\mathrm{Im}(\hat{\epsilon}_2)}{1+n_3}. \tag{5}$$

Even in the case of thin substrates (including backside reflection) this proportionality will hold, whereas in case of thick

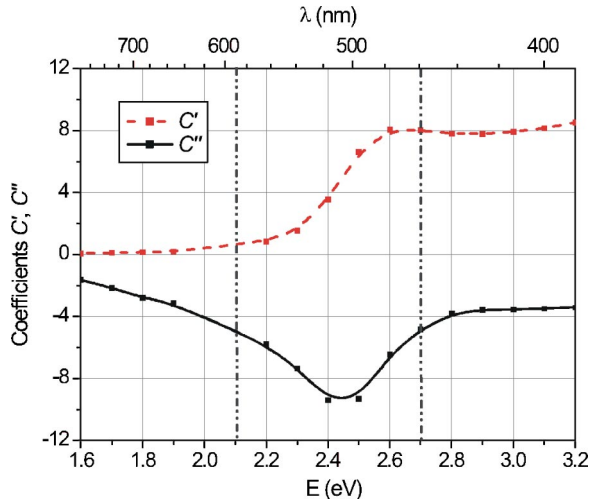

FIG. 3. (Color online) The coefficients C' and C'' for Au as substrate. Two different spectral regions $E<2.1$ eV with $C'\approx 0$ and $E<2.7$ eV with $C'\approx -2C''$ can be distinguished, representing two limiting cases of the $\Delta R/R$ signal composition. For comparison, in the case of mica the coefficients have the values of $C'\simeq 0.005$ and $C''\simeq 40$ at 2.6 eV, hence the influence of $\mathrm{Re}(\hat{\epsilon}_2)$ on the DRS signal can be neglected.

films the optical density is proportional to the absorption coefficient $\alpha_2=(2\omega/c)\mathrm{Im}(\sqrt{\hat{\epsilon}_2})=4\pi k_2/\lambda$ (Beer's law).

As an opposite example, we discuss gold as substrate. Gold is not only opaque, but also possesses a typical yellowish color, in contrast to, e.g., silver or aluminum. Therefore, one has to deal with strongly varying optical constants in the visible wavelength range. This has a large impact on the $\Delta R/R$ spectra as shown in Fig. 2.[25,26] To quantify this influence, we will further transform Eq. (2) to

$$\frac{\Delta R}{R}\cong d_2\{C'[1-\mathrm{Re}(\hat{\epsilon}_2)]+C''\,\mathrm{Im}(\hat{\epsilon}_2)\}, \tag{6}$$

where the coefficients C' and C'' depend only on the complex dielectric function $\hat{\epsilon}_3$ of the substrate, but not on $\hat{\epsilon}_2$.[28]

In case of the substrate gold, those coefficients C' and C'' vary rather strongly over the wavelength range of the measurement (Fig. 3). Only within the low-energy range, the $\Delta R/R$ signal corresponds approximately to the absorption where $\Delta R/R\propto -\mathrm{Im}(\hat{\epsilon}_2)=2n_2k_2$, because C' is small. On the other hand, in the energy range $E\geqslant 2.7$ eV, Eq. (6) simplifies to $\Delta R/R\propto n_2(n_2-k_2)-1$, here $-C'$ is approximately twice as large as C''. Therefore, the DR spectra can be directly related to the absorbance spectra in the low-energy range only.

III. *IN SITU* SETUP

A. Optical system

The optical *in situ* setup is implemented in a 3 chamber OMBE system described elsewhere.[29] It is intended to be UHV compatible and to cover a large wavelength range as an universal tool for a large variety of adsorbate systems. A wavelength range of 200 to 1000 nm (corresponding to an energy range of 6.2–1.2 eV) was desired, therefore common

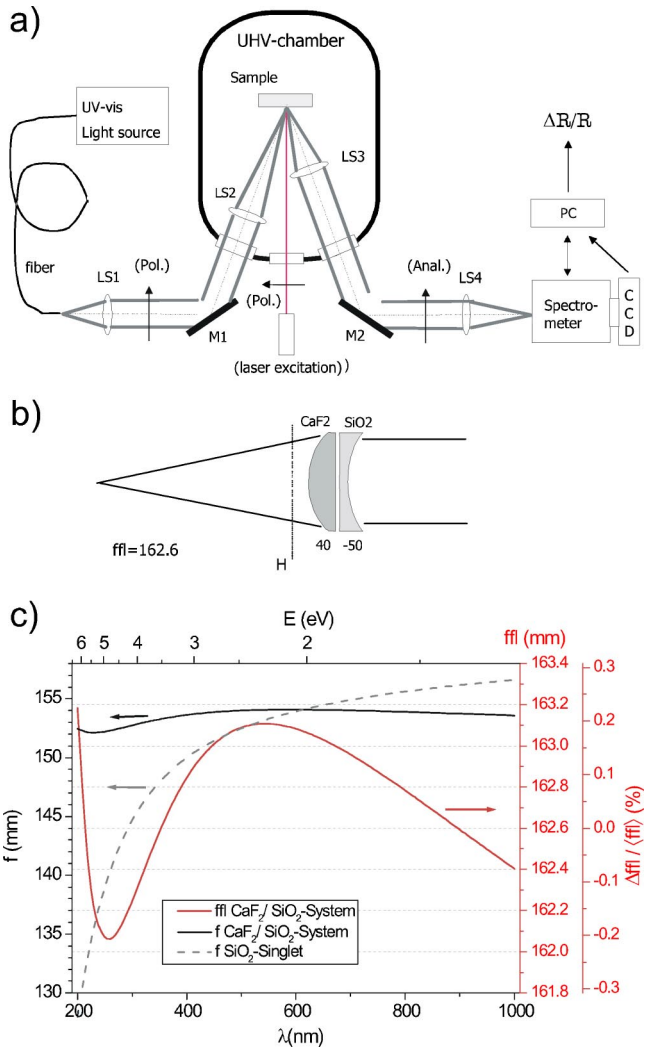

FIG. 4. (Color online) (a) Scheme of the UHV growth chamber with the *in situ* DRS setup. The optical system consists mainly of four lens systems LS1–LS4 and two UV-enhanced Al mirrors M1 and M2. To check for anisotropy, two polarizers (Pol.+Anal.) can be inserted. (b) The lens systems LS1, LS2, and LS4 with a front focal length (ffl.) of about 163 mm consist of two commercial SiO_2 and CaF_2 singlets, while LS3 (not shown here), the system of accumulation, has half the focal length and consists of three singlets. (c) The lowest achievable chromatic aberration of the doublets LS1, LS2, and LS4 in the wavelength range of interest for the optimum lens distances.

achromatic single lenses could not be used. Additionally, we aim at a small detection area on the sample and a large detection steradian, to also enable fluorescence measurements (not shown here). To match this requirements, collimating systems with minimal chromatic aberration and a small distance to the sample are needed. This is achieved by the combination of commercially available SiO_2 concave and CaF_2 convex lenses inside the UHV chamber, moreover allowing an unrestricted bakeout of the system.

Figure 4(a) shows the overall setup. The collimated light beams enter and leave the UHV chamber via SiO_2 Suprasil windows and are focused/collimated by the lens systems LS1–LS4. In Figs. 4(b) and 4(c), a scheme of the lens sys-

tems and the corresponding chromatic aberration are shown. The deviation from optical isotropy caused by the influence of the optical elements is smaller than ±10% in the visible wavelength range. The area of investigation on the sample is about 0.5–0.75 mm^2, the angle of incidence is about 20°.

B. Recording of spectra

An optical multichannel analyzer (OMA) consisting of a grating-mirror spectrograph (Acton Research SpectraPro-150, 300 g/mm blazed grating) with a CCD allows a fast spectra collection. We use a single stage peltier-cooled back-illuminated CCD (Roper Scientific, SpectruMM 250B) with a fast 16 bit AD interface (100 kHz sampling rate). Besides its high sensitivity, it exhibits a relatively large dark noise of ~0.4% (per single acquisition) at maximal possible illumination, caused by a minimal achievable detector temperature of typical −35 °C only. The 16 bit interface limits the counting rate to 2^{16} maximum counts per channel, which implies an additional statistical noise $\Delta N/N=\sqrt{N^{-1}}$ of at least ~0.4% at full load, which further increases at lower light intensities. Compared to that, the noise of the A/D conversion (ten electrons) is negligible.

Therefore, we accumulate the signal of several successive acquisitions (typical 500–1600) to improve the signal-to-noise ratio of ΔR by a factor of approx. 20–40, which is necessary to investigate (sub)monolayers of adsorbed species (see below). Nevertheless, we achieve short measuring times of 20–50 s by a continuous light exposure of the CCD, with no extra delays, hence the exposure time of a CCD line is determined by the read-out time.[30] This enables us to carry out *in situ* real-time measurements during the film growth, with the implication that our spectra represent an average over a certain film thickness range, depending on both the deposition rate and the measuring time (see below).

IV. APPLICATION TO ULTRATHIN PTCDA FILMS

A. Experiment

The PTCDA films were deposited under ultrahigh vacuum (UHV) conditions by evaporation from a low flux Knudsen-type effusion cell at a cell temperature of ~330 °C and a vapor pressure of $\sim 3\times 10^{-9}$ mbar. The evaporation was done after a thorough degassing of the cell at 200 °C. The PTCDA deposition flux was about 0.2 ML molecular layers (ML) per minute and checked by a quartz microbalance. However, the exact growth rate has been determined by optical means (see below).

During and after the film deposition, the substrate was kept at room temperature. For every new experiment, either a freshly cleaved sheet of mica (Ted Pella Inc., Hi-Grade), which was extensively degassed in UHV at 150–180 °C for 1–2 h to remove the water film and other contaminants from the surface, or an Ar^+ sputtered (600 eV) and annealed (600 °C) Au(111) single crystal was used.

The DR spectra were collected with the setup described above. As a source of unpolarized light we used a quartz tungsten halogen lamp. For each spectrum, 1500 successive acquisitions were averaged, corresponding to a total measuring time of about 40–45 s. The spectra were corrected for mechanical drift of the setup and thermal drift of the light source by analyzing the $\Delta R/R$ spectra series obtained before and after the deposition process. In most cases, these series could certify the assumption of a spectral constant drift over time, making a drift correction of the spectra possible. A Shimadzu spectrophotometer (UV-3101 PC) was utilized for the *ex situ* absorbance measurements.

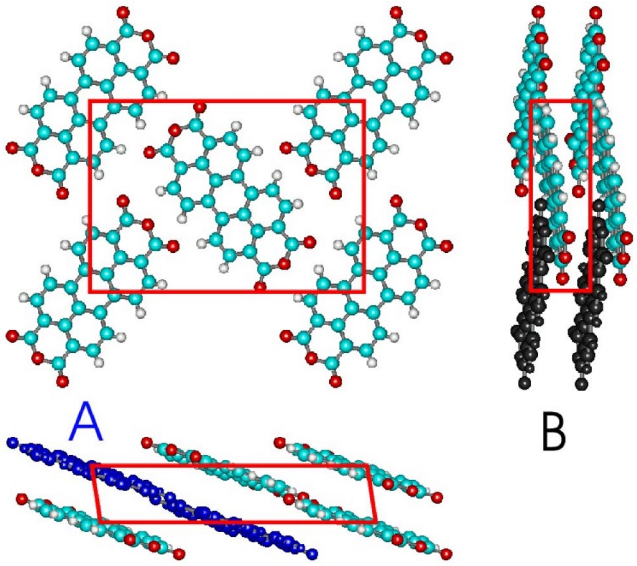

FIG. 5. (Color online) Views of the PTCDA crystal (α modification): (100) plane (top), (001) plane (right), and (010) plane (bottom). A unit cell and the two types of PTCDA dimers, *A* (in plane) and *B* (out of plane, i.e., stacked), are indicated. The unit cell dimensions are $\alpha=3.72$ Å, $b=11.96$ Å, and $c=17.34$ Å. Crystal data were taken from Refs. 31 and 32.

B. Optical spectra and discussion

In this section, we describe and discuss both the $\Delta R/R$- and the absorbance spectra obtained for PTCDA grown on different substrates, after giving a short introduction in the properties of PTCDA single crystals. The PTCDA crystals of both the α and the β modification exhibit a strong anisotropy in their electronic and optical properties due to a densely packed arrangement of the molecules.[1] The interaction in the crystal can be described by discriminating between two types of physical dimers, *A* and *B*. The molecules in the *A* dimers, building up the crystal (102) bulk plane, are arranged in the herringbone (HB) structure as predominantly found in ultrathin PTCDA films, and interact rather weakly. The molecules in the π-stacked dimer *B* exhibit a large magnitude of interaction. Those nearly perpendicularly arranged molecular stacks represent "molecular chains" and dominate the optical and electronic properties of the highly anisotropic PTCDA crystal (compare Fig. 5).[33] Therefore, PTCDA can be regarded as a quasi-one-dimensional crystal. From exciton theories, it is known that the properties of such one-dimensional stacks depend strongly on the chain length, where a chain length of 4 already approximates an infinite chain quite nicely.[16] Hence, we expect a strong dependence

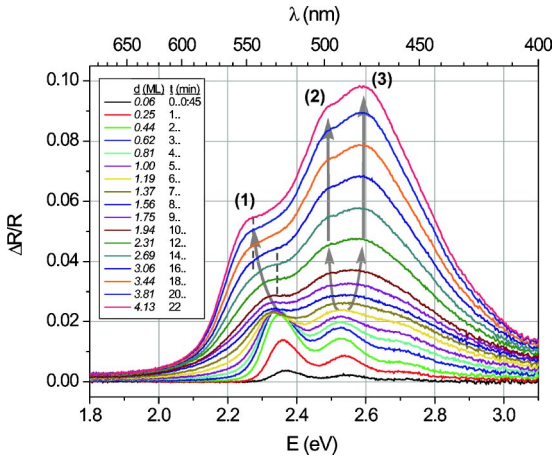

FIG. 6. (Color online) The differential reflectance spectra of PTCDA on mica during film growth, from 0 ML to a final film thickness of 4.1 ML. During one measurement the increase of the layer thickness is about 0.12 ML, therefore 0.06 ML will read 0–0.12 ML. Note the clear change in the characteristic spectral shape and the two intersection points at about 2.30 and 2.35 eV.

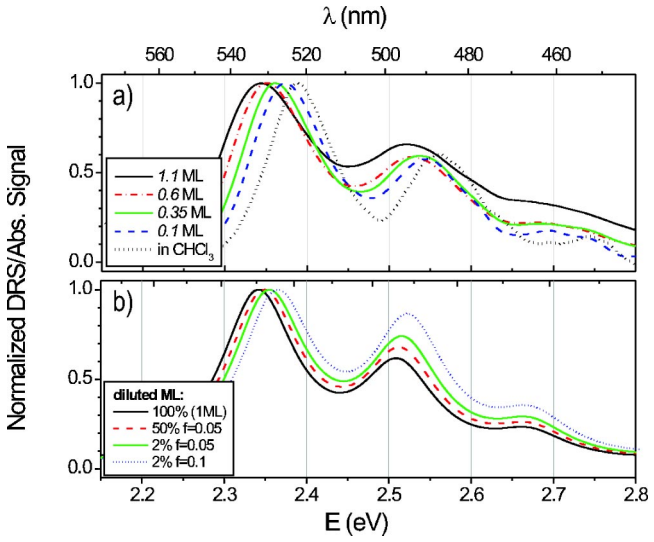

FIG. 7. (Color online) (a) The normalized differential reflectance spectra of PTCDA on mica in the thickness range of 0.06–0.8 ML, and the normalized absorbance spectra of PTCDA dissolved in $CHCl_3$ for comparison. (b) Simulated normalized DRS spectra in dependence on the monolayer completion in the described effective medium model with an assumed form factor f of 0.05 which corresponds to distributed PTCDA islands of about 5 nm diameter embedded in vacuum down to isolated molecules with $f \sim 0.1$. With increasing island size, f decreases and the influence on the spectra diminishes with respect to the closed monolayer.

of the absorption spectra on the layer thickness in the experimental range investigated in this work.

1. PTCDA on mica

Muscovite mica, $KAl_2(Al,Si_3)O_{10}(OH)_2$, is an easy cleaveable sheet silicate, transparent in the visible. After cleavage, one obtains many square microns of atomically flat (0001) surfaces, with a surface mesh of a ~5.25 Å lattice constant. The almost inert mica surface is well suited as a substrate for deposition studies; here the reader is referred to literature, i.e., Refs. 34–36.

a. DRS. The DR spectra in Fig. 6 show a strong change of the spectral shape with increasing film thickness. The spectra up to 4 min deposition time (~0.8 ML film thickness) are comparable to the absorption of PTCDA in solution [see Fig. 7(a)]. The two recognizable peaks at 2.35 and 2.55 eV, and the feature around ~2.75 eV belong to the energetically lowest (S_0-S_1) transition, separated by a vibronic progression of $\Delta E \sim 0.17$ eV.[13,15] A simultaneous shift of the prominent peaks to lower energies by ~29 meV (redshift) with increasing coverage occurs, shown in more detail in Fig. 7(a). These shifts, comparable to solvent shifts, were already explained by an increased dielectric screening with increasing coverage in Ref. 17, and were also observed for amorphous layers of PTCDA.[37] The Davydov splitting, caused by the translationally nonequivalent molecules in the unit cell, i.e., the *A* dimers (compare Fig. 5), cannot be observed directly. It will affect the spectra of the monolayer only via its contribution to the overall broadening of the spectra, due to the fact that its value of 10–35 meV,[33,38] compared to the width of the bands, is by far too low to be resolved in our room temperature experiment.

Here, we want to show that the observed peakshifts can be already quantified by a classical local field approach. We consider the growing molecular film as an inhomogeneous mixture of molecules and vacuum. Its optical properties are then described by an effective dielectric constant. The microscopic components itself modify locally the external applied external field, provided by the electromagnetic wave of the light. The interaction of the components with those local fields finally define the optical properties of the composite, which are therefore considered to be determined only by the dielectric functions of its components. This polarization-induced effects will occur in general in mixtures of two or more species, which are in our case PTCDA and vacuum. If island growth would occur, effects due to the shape of the mixed "particles" have to be considered as well. These (purely optical/electromagnetic) effects can be well described by effective medium theories (EMT), and we shall discuss whether such effects can explain the observed redshift of the spectra in Fig. 7(a).

The application of an EMT to explain optical spectra of thin inhomogeneous films and island growth was demonstrated by David,[39] who used a simplified model for low coverages, in which the shape of the particles was accounted for by its anisotropic depolarization factors $f^{(i)}$. The following expression of the effective dielectric functions $\langle\hat{\epsilon}\rangle$ of particles of the materials 1 and 2 ($\hat{\epsilon}_1, \hat{\epsilon}_2$) embedded in the host material ($\hat{\epsilon}_h$) given by

$$\frac{\langle\hat{\epsilon}\rangle - \hat{\epsilon}_h}{\langle\hat{\epsilon}\rangle + Y_h\hat{\epsilon}_h} = q_1\frac{\hat{\epsilon}_1 - \hat{\epsilon}_h}{\hat{\epsilon}_1 + Y_2\hat{\epsilon}_h} + q_2\frac{\hat{\epsilon}_2 - \hat{\epsilon}_h}{\hat{\epsilon}_2 + Y_1\hat{\epsilon}_h} \tag{7}$$

leads to the EMT of Maxwell-Garnett[40] for the choice $\hat{\epsilon}_h = \hat{\epsilon}_2$ as well as to the self-consistent theory of Bruggeman[41] for $\langle\hat{\epsilon}\rangle = \hat{\epsilon}_h$, with q_i the quantity (volume or area fraction) of

the material i whose particle shape is accounted for by $Y_i = (1/f_i - 1)$. Here, f_i corresponds to the depolarization factor in the direction of the incidence of light, leading to $f_i = 1/3$ for the isotropic case (spheres).[42]

To model our system, we start with a complete monolayer of molecules and dilute it. The DF of one PTCDA-monolayer $\hat{\epsilon}_{1\ \mathrm{ML}}$ is derived from the DR spectra for a complete monolayer film by using a Lorentz oscillator model (LOM) for $\hat{\epsilon}$.[43] Utilizing this dielectric function $\hat{\epsilon}_{1\ \mathrm{ML}}$ of a monolayer, the calculated spectra of a diluted film of monomers with disklike islands (corresponding to small f_i values) are shown for the Maxwell-Garnett case in Fig. 7(b). It is clearly visible that a redshift of the monomer spectrum occurs during completion of the monolayer.[44] For the considered island diameter of about 5 nm, the spectral redshift of about 20 meV reflects the result of the experiment nicely. If larger islands are assumed to grow on the sample, the influence of the molecule concentration or layer completion on the spectra is reduced, i.e., the largest shifts will occur in the very beginning of the deposition. Two limiting cases of growth modes are imaginable, depending on the deposition flux and the mobility of the molecules on the mica substrate: during layer deposition either the size of a constant number of island increases (the molecules wet the surface), or the number of many small distributed islands increases until the layer is completed. The latter case should be more likely on a cooled substrate while the first growth mode should dominate at room temperature. Measurements carried out on a LN_2-cooled mica substrate ($T \sim -160$ °C) showed that already at smallest coverages, the monomeric absorption vanishes in favor of the dimer spectrum (not shown here). Due to reduced mobility/diffusion of the molecules, the surface is not wetted anymore before the second molecular layer starts to grow. Hence, we can assume wetting of the mica surface for deposition on substrates kept at room temperature. The degree of wetting will be discussed in the next paragraph.

At a nominal thickness of ~1.2 ML, the ratio of the two prominent energetically lowest peaks has already changed. Despite ongoing deposition, the height of the spectrum does not grow proportionally anymore, but *Peak1* shows a small shift downwards in energy (redshift) and becomes weaker and broader. Additionally, the spectrum crosses that one of 0.8 ML coverage at fixed positions. These so-called isosbestic points are a characteristic behavior in the absorption spectroscopy of an equilibrium of two absorbing species $X \rightleftharpoons Y$.[46] As reported in Ref. 17, we identify the species X and Y with the PTCDA monomer and the stacked PTCDA dimer, respectively. In the $\Delta R/R$ spectra shown in Fig. 6 these points can not be observed for all spectra in the thickness range between 1 and 2 ML, in contrast to the spectra shown in Ref. 17. The reason is a different "quality" of the layer-by-layer growth depending critically on the sample surface and treatment, as will be shown in the following.

To discuss the material's properties, we want to focus on a thickness independent quantity. Therefore, in Fig. 8 we plotted $\mathrm{Im}(\hat{\epsilon})$ as it was estimated from the $\Delta R/R$ spectra of Fig. 6 using Eqs. (3) and (4). Isosbestic points or at least nearly isosbestic behavior can be observed in four regions. In the $\mathrm{Im}(\hat{\epsilon})$ spectra in Fig. 8, two isosbestic points at 2.27 and 2.77 eV persist with increasing coverage, once the transition from monomer to dimer (and oligomer) has started, while the intersection points at 2.41 and 2.62 eV are not shared by all spectra. At 2.41 eV only the spectra of ~1.4 to 1.9 ML, and at 2.62 eV the spectra from 0.8 to 1.4 ML coverage intersect. This would further confirm the assumption of layer-by-layer growth characterized by a stepwise transition from monomer to dimer to trimer,[47] hence the isosbestic point at 2.41 eV should be the result of the transition from the dimer to the trimer of PTCDA, and the intersection at 2.62 eV would be due to the monomer dimer transition. The monomerlike spectra up to a deposition time of 3 min do not intersect at 2.27 and 2.77 eV, hence the building of dimers just starts if already large molecular islands are grown on the sample. The stepwise occurrence of isosbestic points implies a coexistence region between *A* dimers (behaving like monomers) and *B* dimers (behaving like a new species which we simply call "dimers" herein for short), and later on of dimers and trimers. This is a clear indication that layer-by-layer growth dominates, although the first monolayer seems not to be entirely completed before the dimer starts to grow (compare with DRS spectra shown in Ref. 17). In this respect, the growth of PTCDA on mica differs from metal surfaces, as will be shown below. These different growth modes also have an impact on the observation of isosbestic points in the

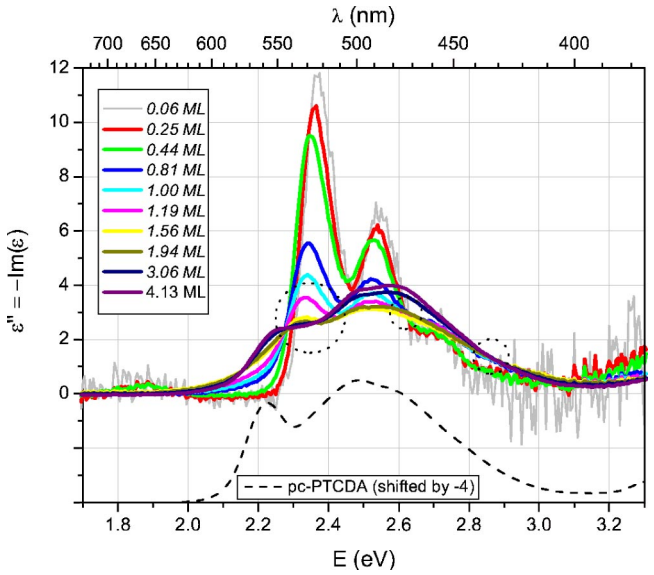

FIG. 8. (Color online) $\mathrm{Im}(\hat{\epsilon})$ spectra estimated from the differential reflectance spectra of PTCDA on mica, which were recorded with a constant molecular flux of about 0.2 ML/min, from 0 to 12 min (see text, corresponding effective film thickness 0–2.3 ML). Intersections of spectra can be found at about 2.27, 2.41, 2.62, and 2.77 eV, as indicated. For comparison, the $\mathrm{Im}(\hat{\epsilon})$ of thick polycrystalline films as reported in Ref. 27, is also shown in the bottom (shifted). We believe that the spectral feature at ~1.87 eV in the submonolayer spectra stems from charged molecules, since mica(0001) exhibits a slightly polar surface (Ref. 34). This would imply a transition energy of ionized PTCDA lowered by ~50 meV compared to the neutral molecule, and fits well to studies of neutral and ionized perylene (Ref. 45). A similar feature was also reported by Bulovic *et al.* (Ref. 13) in the absorption of PTCDA dissolved in the strongly polar *N*-methylpyrrolidone (NMP).

$\Delta R/R$ spectra. For the ideal case of a complete first layer, every additional molecule causes the transformation from a monomer to a dimer. This leads to the clear appearance of isosbestic points in the $\Delta R/R$ spectra. On the other hand, for uncompleted first layers, the oncoming molecules can still contribute to the monomer spectrum, so that the condition for the observation of isosbestic points in the $\Delta R/R$ spectra $(1X \rightarrow 1Y)$ is not fulfilled. Hence, the balance between the diffusion rate of the molecules on the first monolayer (compared to those on the bare mica surface) and the deposition flux is crucial. We found experimentally that the quality of the layer-by-layer growth regime depends very sensitively on the mica surface preparation. If we have a large mobility of the molecules on mica, large monomer islands will grow on the surface. In that case, a large amount of dimers will already start to grow at a lower nominal PTCDA coverage (a large diffusion path of molecules on top of the island is required to reach the island boundary). We could find this behavior in the case of unannealed mica substrates. There, the spectra have strong aggregate contributions already at a nominal coverage of 0.44 ML and show a shape comparable to thick or polycrystalline films from 0.6 to 0.8 ML on (not shown here). Due to the fact that the mica surface is slightly hydrophilic,[36] we assume a film of adsorbed H_2O molecules to strongly enhance the mobility of the PTCDA molecules (compare with the findings in the absorbance measurements, next section). Vice versa, if we have much lower mobility on the mica surface, compared to the mobility of PTCDA on the islands, we will find a large number of smaller islands on the sample, and the dimer will occur at a higher nominal deposition amount.

With increasing PTCDA coverage, the spectral shape changes further and resembles finally the spectra known for thick polycrystalline PTCDA films (compare Refs. 27 and 33). This process is more or less finished at a coverage of 4 ML, as can be seen in Fig. 6. The low-energy feature *Peak1* at 2.32(6) eV and two features at higher energies become more pronounced (*Peak2* at 2.48 eV, *Peak3* at 2.57 eV). Additionally, *Peak1* shifts downwards in energy by ~60 meV.

To further prove the above interpretation, we plot the $\Delta R/R$ signal integrated over the interval [2–3] eV (S_0-S_1 transition) versus the deposition time, as shown in Fig. 9. Expecting a constant flux in our experiment, this quantity is proportional to $\int \mathrm{Im}(\epsilon) E dE$, a measure of the (observable) oscillator strength of the transition.[48] It can be seen that, except for the range of 0.8–2 ML, the curve has a constant slope indicating a constant increase of the oscillator strength in the layer. Because the slope is the same for the thick layers as for the (sub)monolayers, the corresponding oscillator strength per molecule in this films is equivalent. From the slope in the highest thickness region, we were able to more precisely determine the flux of the PTCDA deposition by simulating $\Delta R/R$ of PTCDA films on a mica substrate with the optical constants of PTCDA derived for thick films.[27] Here, the thickness of the mica substrate of the respective sample (Fig. 6) was determined from OD measurements to be 190 μm, using optical constants of mica from Ref. 49. A refined value of the total final film thickness of the sample was estimated to 4.1 ML, finally leading to a value of ~0.2 ML/min for the PTCDA flux. Furthermore, it can be

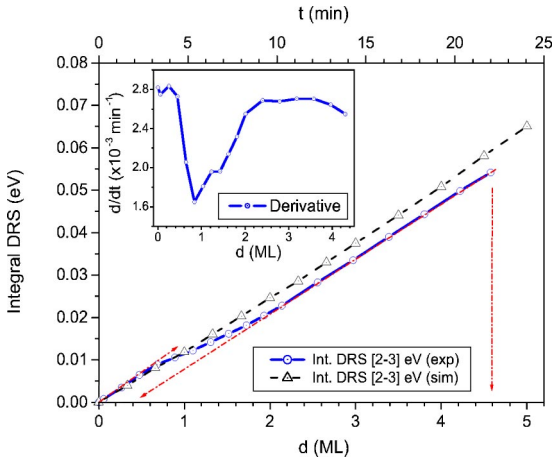

FIG. 9. (Color online) Experimental integral DRS of the sample from Fig. 6, and simulated integral DRS of PTCDA on mica (190 μm), using the optical constants of polycrystalline PTCDA (Ref. 27). The integration interval was 2–3 eV in correspondence to the position of the S_0-S_1 transition. The demand of equal slopes of the simulated and experimental curve in the higher thickness region allows to refine the final film thickness, being estimated to 4.1 ML. In the inset, the derivative of the experimental integral DRS is plotted. A decreased (observable) oscillator strength per molecule (hypochromism) in the thickness interval of ~1–2 ML is clearly visible.

seen in Fig. 9 that the linear approximation for $\Delta R/R$, first given by McIntyre and Aspnes,[21] is valid even in the thickness range up to 5 ML.

At a first glance one might attempt to explain the decreased slope in the thickness range of 1–2 ML by a redistribution of oscillator strength within the energy interval 2–3 eV to charge transfer excitons (CTE). These kind of excitons can exist only if the second layer starts to grow and exhibit transition dipoles which have a large component out of the molecular plane, leading to a reduced oscillator strength per molecule. However, this is in fact rather unlikely since the relative oscillator strength attributed to charge transfer excitons is only about 2–3%.[15,50]

The occurrence of hypochromism in the thickness range of ~1–2 ML coincides with the observation of the isosbestic points in the spectra (compare Fig. 6). If the layer is growing further, the oscillator strength per molecule is again similar to the value of the isolated molecules (as found in the monolayer). We explain this behavior by on-site effects caused by the special arrangement of the molecules in the molecular crystal: It is known from comparative investigations of DNA-nucleotide and -polynucleotide chains that a parallel arrangement of transition dipoles lead to an reduced observable absorption (beyond a blueshift of the transition energies), i.e., hypochromism, if more than one transition is considered while a head-to-tail arrangement will lead to an absorption increase (hyperchromism).[51,52] This can explain as well the here observed hypochromism in case of the stacked PTCDA dimer after the second molecular layer starts to grow, an interpretation which is further confirmed by investigations of perylene sandwich dimers.[53,54]

A further increase of the PTCDA film thickness is coupled with a further enlargement of the molecular chains built of

stacked PTCDA molecules, although no additional type of interaction comes into play. Here, we have to keep in mind that on-site effects like the shift of the transition energies due to a reduced number of nearest neighbors in the outermost molecular layers of the film were used to explain effects like the blueshift of absorption in case of ultrathin films (see below).[10,17] Those shifts of absorption energies can be understood classically by a decreased dielectric screening in the outermost molecular layers. However, we have to remind that a reduced background dielectric screening also decreases the observable oscillator strength of a certain transition.[48] It is generally acknowledged that the dielectric constant of a bulk crystal develops at length scales comparable to the nearest-neighbor-distances, in our case the stacking distance.[9,50] Hence, in case of a stacking length of already $N \geqslant 3$, we can consider for the innermost molecules a dielectric screening like in the bulk material. If the PTCDA chain length exceeds $N=3$, the number of innermost molecules increases, showing a stronger absorption compared to the outermost molecular layer. In our case, the resulting slope of the $\int \Delta R/R dE$ curve becomes steeper and corresponds (within the limits of the experimental accuracy) to the slope in the submonolayer region.

Due to the fact that the slope of the curve of the experimental DRS does not significantly decrease with increasing film thickness, we can exclude an increased roughening of the film up to a thickness of 4 ML.

b. Absorbance. To relate the *in situ* DRS results to a common method and other reported results, the samples of different final thickness were transferred out of the UHV system to measure their absorbance *ex situ*. The differential optical density of the PTCDA film was estimated by subtracting the absorbance of the mica substrate (as measured before transferring them into UHV) from the film covered sample.

The shape of the absorbance spectra is equivalent to the DRS spectra in case of films thicker than 2–3 ML as can be seen in Fig. 10. With decreasing thickness, even if the films become as thin as 1–2 ML, the absorbance spectra keep their polycrystalline character. This suggests that the film is reordering at ambient conditions while transferring the sample to the transmittance measurement setup. The catalyst seems to be a film of adsorbed water, which stems from the atmospheric moisture. To prove this assumption, the sample was rapidly transferred to the spectrophotometer by using an exsiccator, after venting the transfer load lock with dry nitrogen. The transmittance was then measured in the spectrophotometer which was previously prepared with desiccant, too, to reduce the humidity inside. The time dependence of the absorption spectra could therefore be resolved and is shown in Fig. 11, which confirms the assumption proposed above. Due to clustering, not only *Peak1* but the overall OD is reduced, as can be seen in Table I.[56] For films thicker than 2 ML, no time dependence of the transmittance on these time scales could be observed. Nevertheless, a comparison of the thickness values of the films with the highest final coverages in Table I shows a slightly lower *ex situ* absorbance than expected, leading to the assumption that at ambient conditions additional roughness due to clustering at the film surface may occur.

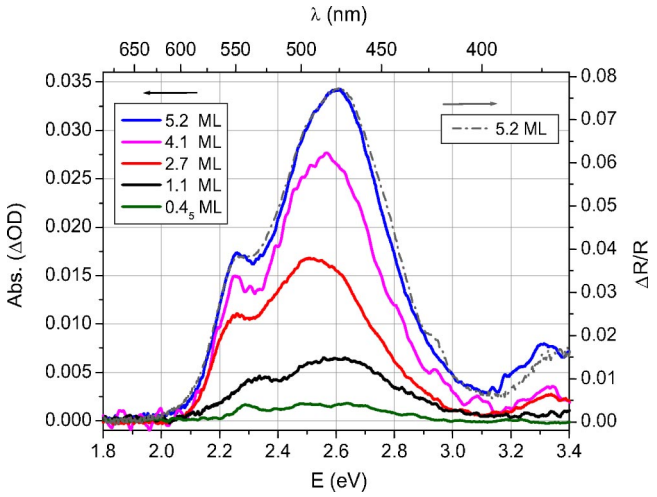

FIG. 10. (Color online) The absorption spectra (ΔOD, left *y* axis) of investigated PTCDA on mica films with different final thickness from 0.4 to 5.2 ML. In case of the 5.2 ML sample the $\Delta R/R$ spectrum is shown for comparison (right *y* axis). The differential optical density of the films was determined by the difference of the optical density of the sample before and after film deposition. The shape of the ΔOD spectra remains constant even when the nominal film thickness becomes as thin as 1 ML.

In Fig. 12, the shift of *Peak1* in both DRS and absorbance is plotted versus the film thickness. Two different slopes of the shift can be clearly identified. With decreasing thickness down to 4 ML, only a small shift of about 40 meV of *Peak1* occurs, whereas in the coverage range of 3–1 ML it extends to ~65 meV. The shifts in OD and DRS are very well comparable, except for the thinnest films. In this case, *Peak1*

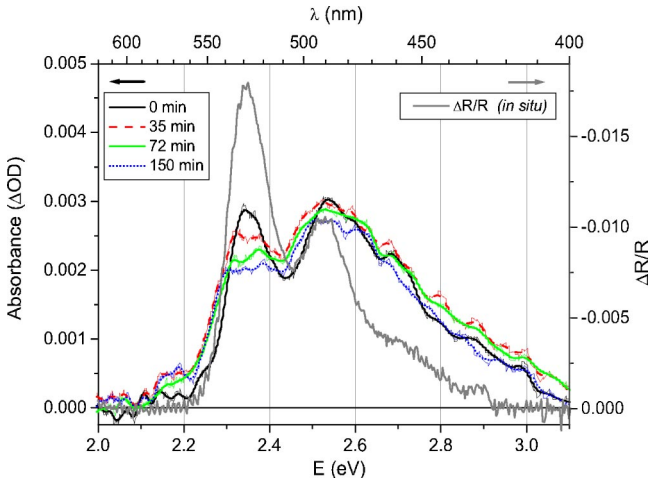

FIG. 11. (Color online) The time dependence of the ΔOD spectra of ~0.75 ML PTCDA in a desiccated spectrophotometer. The time $t=0$ corresponds to the first measurement after the transfer from the vacuum lock into the spectrophotometer in an exsiccator (the duration is ~3 min). The spectra were noise filtered by the method of Lee (Ref. 55) (window size=5). Due to the small thickness of the mica substrate, small interference modulations are visible in the spectra. In measurements after 24 h (not shown here), *Peak1* was found redshifted by 17 meV. For comparison, the $\Delta R/R$ signal of the sample is also shown (gray line, right scale).

TABLE I. Final nominal film thickness d_{dep} of different samples as deposited, and estimated effective thickness d_{OD} from the integrated *ex situ* absorbance (ΔOD) spectra (accuracy about 10%). Note that for the thinnest film the optically estimated thickness is below the expected value, due to reordering (see text).

d_{dep} (ML)	$\int \Delta OD\, dE$ (cm^{-1} eV)	d_{OD} (Å)	ML
0.7_5	0.0015	1.41	0.4
1.1_5	0.0039	3.36	1.0_5
2.4	0.0087	8.20	2.5
4.1	0.0138	13.0	4.0
5.2	0.0174	16.4	5.0

shifts further to the red, due to the aforementioned reordering processes at ambient conditions, leading to clusters with larger PTCDA "chain lengths." In summary, absorbance and DR spectra are similar with respect to the main features and spectral shifts, but differ in details arising exclusively from the ambient conditions in which the absorbance measurements were done.

We now discuss in more detail the origin of the peak shifts observed: The observed shifts are in accordance with other experiments, but somewhat larger: So *et al.*[57] reported peak shifts of the lowest absorption maximum of about 25 meV for PTCDA/NTCDA (Ref. 58) multiple quantum well (MQW) structures with decreasing well width, varying from 200 to 10 Å (65–3 ML) layer thickness per well. A blueshift of about 80 meV can be obtained from transmission spectra of MQWs made of stacked PTCDA/InPc-Cl (Ref. 59) layers with decreasing PTCDA well widths of about 250 to 3 Å (80 to 1 ML), investigated by Anderson and co-workers.[60] Due

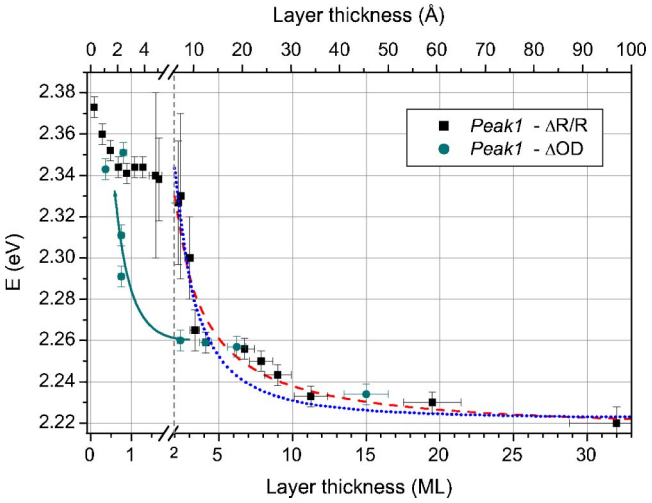

FIG. 12. (Color online) The shift of the low energy feature *Peak1* (uncertainty indicated by error bars) in $\Delta R/R$ and in absorbance (ΔOD) spectra at different final film thicknesses of PTCDA on mica. In the case of the absorbance, a large shift is already observed at lower film thicknesses (<4 ML), due to reordering and clustering of the films in ambient conditions. The dashed curve shows the fit with an on-site-effect model (Ref. 10) (d^{-1} dependence), while the dotted line corresponds to a fit with an simple exciton confinement model ($\sim d^{-2}$-dependence). For details see text.

to the relatively large total thicknesses of that OMBE-grown MQWs (well numbers of 5–20), inevitable surface roughness will cause nonideal interfaces and nonuniform well thicknesses, which will finally lead to a superposition of the spectral characteristics of different PTCDA chain lengths. Especially in case of the thinnest well widths, where we expect the most drastic changes, the shifts will smear out. Peak shifts around 60 meV were also reported for fluorescence excitation spectra of PTCDA layers of 3–80 ML thickness by Leonhardt *et al.*,[12] but were explained by the superposition of the slight different absorption of the PTCDA α and β phase.

The observed shifts were already previously interpreted by exciton confinement[9,61] or local field effects.[10,11] Here, we want to compare this two approaches. A relatively small intermolecular distance in the PTCDA stacks of $d_{ML}=3.38$ Å could allow a strong intermolecular interaction, leading to an exciton delocalized over the molecular stack. Hence, one could consider the exciton being confined in a (one-dimensional) potential well. The dimension L of the well, represented by the chain of N stacked molecules, is given by $L=(N+1)d_{ML}$, if we assume that the exciton wave function vanishes at the next lattice points outside the chain. Already the model of an infinite one-dimensional quantum well, characterized by the ground state energy

$$E = \frac{\hbar^2 \pi^2}{2m_{\text{eff}} L^2} + E_0 \tag{8}$$

can fit the data, leading to an effective mass of $m_{\text{eff}} \approx 3m_e$, as can bee seen in Fig. 12.[62] Here, m_e stands for the electron rest mass, and the energy value for an infinite chain, E_0, can be estimated to $E_0=2.22$ eV. Another approach is to consider a blueshifted absorption in the outermost molecular layers due to on-site effects as it was proposed by Agranovich *et al.*[10] The shift can be understood as a decreased solid state shift caused by the reduced number of nearest neighbors, or in the continuum approach by a decreased dielectric screening for molecules sitting in the surface layers (see above). In this case, the peak position is given by

$$E \approx E_0 + 2\Delta/N. \tag{9}$$

In Ref. 17, it was already shown that this assumption yields a reasonable good fit with the parameters $E_0=2.21_5$ eV, $\Delta=0.11_5$ eV. Here Δ represents the energetic shift of the transition energy in the outermost molecular layer with respect to the bulk transition energy E_0. Whereas the amount of the on-site shift Δ appears large compared to previously reported values,[10] it reasonably compares with recent DFT-based calculations of Vragović.[63] The obtained value of E_0 reflects nicely the position of the low energy peak in case of thick layers (2.22 eV for 30 ML film) and corresponds to the position of *Peak1* in $\text{Im}(\hat{\epsilon})$ obtained from the optical constants for polycrystalline PTCDA.[27] Hence, this on-site-effect model not only results in a slightly better fit (see Fig. 12), but it can also explain intuitively the dependence of the observable oscillator strength on the film thickness, as we have shown above.

c. Spectral shapes: Comparison with theory. In this para-

graph, we want to compare the shape of the spectra, especially of the stacked PTCDA dimer, with the spectra obtained by recent model calculations. As we described above, already the PTCDA stacked dimer (*B* dimer) has a spectral shape near that of the (thick) film. This surprising finding can be related to an early publication of Ferguson:[53] He investigated sandwich dimers of perylene (the unit corresponding to the chromophore core of PTCDA) and found drastic spectral changes between the monomer and the dimer absorption, the latter already resembling the absorption of the molecular crystal in β modification.[64] This can support our findings in case of PTCDA, where to our knowledge no spectroscopic investigations of defined aggregates exist. Investigations of linearly arranged perylene chromophores (interconnected perylene-mono-carboximide units), reported by Christ *et al.*,[65] showed an absorption with the spectral shape of a corresponding monomer, but slightly redshifted, as expected for a head to tail arrangement of transition moments. This confirms the finding of a weak interaction in the PTCDA monolayer, yielding to a monomeric spectral shape.

A microscopic calculation of the spectroscopic properties of PTCDA ultrathin films was presented by Vragovic in Ref. 63. This description, originated from a pure Frenkel exciton model for the PTCDA crystal[14,50] is based on DFT-derived parameters including on-site shifts, and yields the $\mathrm{Im}(\hat{\epsilon})$ shown in Fig. 13(a). The spectral changes occurring with increasing film thickness are obvious, but the transition from monomer to the thin film spectra occurs in a thickness range much larger than observed here. Hence, the in-stack interaction seems to be underestimated. Additionally, the spectrum of the PTCDA monolayer is too much broadened, compared to the experiment, indicating an overestimated in-plane interaction. This broadening also results in a decreased peak height of the 1 ML spectrum and hinders isosbestic behavior in $\Delta R/R$ for the monomer dimer transition [compare Fig. 13(a), dashed line].

Another model description of the PTCDA absorption was introduced by Hennessy *et al.*[66,67] They could explain all spectral characteristics of the PTCDA absorption already in the framework of a Holstein model of the (stacked) PTCDA dimer, including both, Frenkel- and charge-transfer excitons. This would correspond to the strong spectral differences between the monomer and the dimer spectra in our measurements, the latter already resembling nearly the PTCDA thin film absorption. The $\mathrm{Im}(\hat{\epsilon})$ spectrum obtained by Kramers-Kronig analysis from the simulated absorption spectrum in Ref. 67 can be found in Fig. 13(b), besides the monomer spectrum.[68] If similar oscillator strength of monomer and dimer is anticipated for simplicity, it can be seen that isosbestic behavior in $\mathrm{Im}(\epsilon)d \propto (\Delta R/R)\lambda$ will result.

Finally, we will discuss the effect of roughening on the spectra of thin films, because at the highest coverages investigated here, island growth cannot be excluded. To check whether roughness has an impact on the optical spectra, we modeled the DRS spectra of films with different surface roughness. For that purpose, a PTCDA layer with an average thickness of 2 nm (6 ML) was composed of a 1 nm thick solid and a rough surface layer on top of it. This surface layer is represented by a 2 nm thick film of 50% PTCDA (and 50% vacuum) with different particle shapes, described

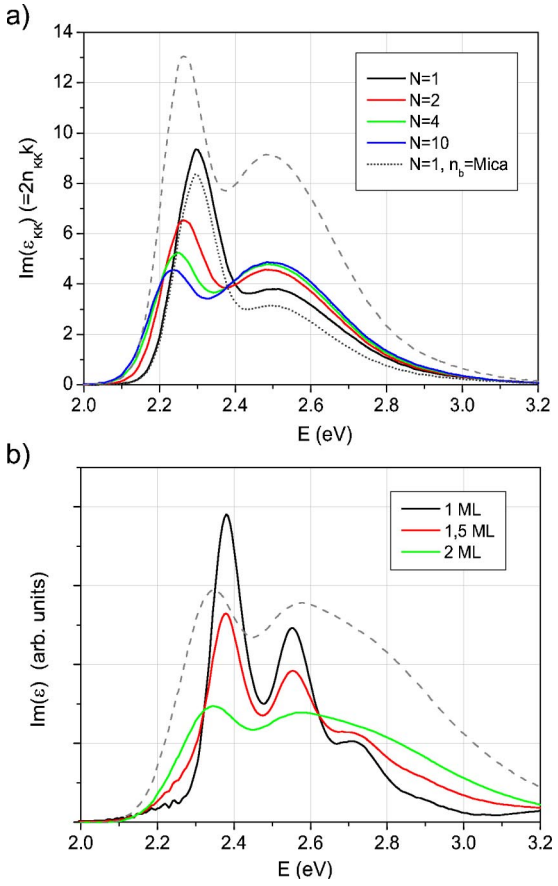

FIG. 13. (Color online) (a) $\mathrm{Im}(\hat{\epsilon})$ spectra of PTCDA layers with thickness N (ML) obtained by Kramers-Kronig analysis from the $\mathrm{Im}(\hat{n})$ spectra given in the work of Vragovic (Ref. 63). In case of the monolayer, we also assumed a reduced dielectric background for PTCDA when calculating the $\mathrm{Im}(\hat{\epsilon})$ spectrum, given by the mica substrate with $\epsilon_b = 2.6$. For the dimer additionally the curve $2 \times \mathrm{Im}(\epsilon)$, corresponding to $(\Delta R/R)/E$, was plotted as a dashed line. Obviously, no isosbestic behavior would be found in DRS. (b) The monomer dimer transition according to Hennessy *et al.* (Ref. 67). In contrast to the original work, we used here $\mathrm{Im}(\hat{\epsilon})$ obtained from the modeled absorbance spectrum via Kramers-Kronig analysis, and we blueshifted the modeled spectrum by 0.11 eV, to fit the experimental position of *Peak1* for the dimer. For the dimer, also $2 \times \mathrm{Im}(\epsilon)$ was plotted as dashed line, resulting in isosbestic behavior even in DRS.

by an EMT with different form factors (see above). In Fig. 14, the resulting DRS spectra in the framework of the EMT of Maxwell-Garnett are shown. The form factor $f = 0.33$ corresponds to spherelike particles, $f = 0.1$ corresponds to (oblate) disks, about eight times larger in diameter than in thickness, while $f = 0.05$ corresponds to oblates with a diameter-to-thickness ratio of about 25. It is obvious that with increasing roughness both, the height of the spectra and their shape, are affected. With increasing form factor f, the spectra change obviously: *Peak3* becomes more pronounced than in the closed layer (for $f \to 0$, we would reach the case of boundless islands, i.e., the case of a closed surface layer of 1 nm thickness), although its intensity decreases. Already at a small roughness, represented by $f = 0.05$, the ratio of *Peak2* and *Peak3* has changed. This observation would correspond to the different peak ratios in the experimental $\Delta R/R$ spectra,

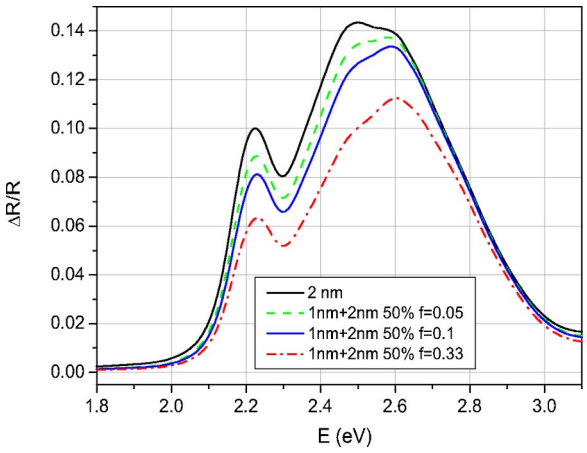

FIG. 14. (Color online) Simulated differential reflectance spectra of 2 nm PTCDA on 150 μm mica, using the optical constants of polycrystalline PTCDA (Ref. 27). The PTCDA layer is either solid or composed of a 1 nm solid layer and a 2 nm layer of 50% PTCDA concentration with different shape factors f to simulate increasing surface roughness, see text. The position of the low energy peak is unaffected; it shows an inessential shift of only ~8 meV to lower energies.

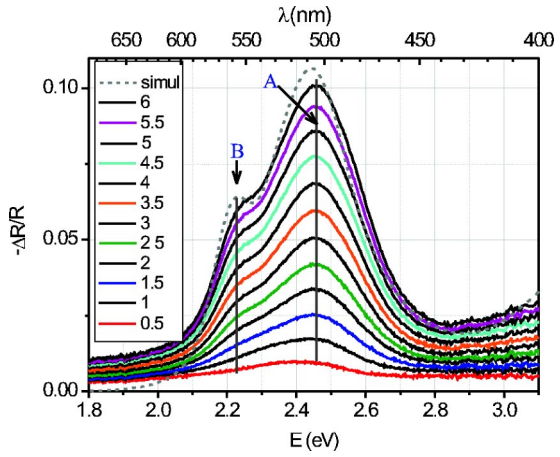

FIG. 15. (Color online) The coverage-dependent differential reflectance spectra of polycrystalline PTCDA on polycrystalline Au, up to a film thickness equivalent to 6 ML. The spectra are characterized by two peaks *A* and *B*, and can be well described by the known optical constants of pc-PTCDA (Ref. 27), as can be seen from the comparison with a calculated spectrum for 2 nm (~6 ML) coverage (dashed line).

an evidence for island growth in thicker layers. We want to mention that surface roughness does not contradict with the assumption of layer-by-layer growth. Ideal layer-by-layer growth means the successive growth of the layers, i.e., the next layer starts to grow not before the underlying layer is closed, leading to an oscillatory behavior of the overall roughness.[69] In the case of the growth of the second ML, the thickness of the rough surface layer amounts to 50% of the total layer thickness. Above, we already stated to expect non-ideal layer-by-layer growth, which would imply on the other hand that the film thicknesses, refined by optically means, are slightly underestimated, while influences of the layer morphology on the position of *Peak1* (as can be appreciated by EMTs) seem to be less important here (compare Fig. 14).

2. PTCDA on Au

In case of the deposition of molecules onto a metal, the increased interaction of the molecules with the substrate should be observable in the spectra. While we have already reported an *ex situ* study of the system PTCDA/Au(111),[25] we want to present here DRS data recorded with the *in situ* setup described. That is giving us the opportunity to exclude reordering effects at ambient conditions modifying the DRS spectra (compare Sec. IV B).

Like on other single crystalline surfaces, PTCDA exhibits highly ordered thin films on gold surfaces, where herringbone and quadratic structures were reported. The findings for PTCDA on Au(111) are described in detail in Refs. 5, 25, 70, and 71.

As a reference, the spectra of polycrystalline (pc) PTCDA films (deposited on pc-Au) are discussed first. From Fig. 15 it is evident that for layer thicknesses larger than 1 ML the spectra remain constant in shape, and can already be completely described by the well-known optical constants of pc-PTCDA.[27] The spectra are characterized by two peaks *A* at 2.46 eV and *B* around 2.22 eV, whose positions for different layer thicknesses remain constant. While the feature *B* corresponds to *Peak1* in the case of PTCDA on mica, feature *A* does neither correspond to *Peak2* nor to *Peak3*. Due to the spectral characteristic of the dielectric function of the Au substrate (compare coefficients C' and C'', Fig. 3), this feature is more or less imprinted in the adsorbate spectra. Its position corresponds nearly to the position of the peak in C''. Therefore, we chose a different labelling for the peaks of the films on Au.

In contrast to the polycrystalline growth, in the case of highly ordered PTCDA on the Au(111) surface a new feature *C* arises at 2.32 eV, starting from a layer thickness of ~1.5 ML, whose intensity is decreasing with increasing layer thickness (Fig. 16). At the same time, the feature *B* which is only weak in the spectra of the very thin layers, becomes more intense with increasing layer thickness. For very thick layers, the spectra of polycrystalline and highly ordered layers look quite similar. The origin of the feature *C* becomes obvious in comparison with the spectra of PTCDA on mica. While in the case of a monolayer of PTCDA on Au(111) the monomer spectrum of PTCDA is very strongly broadened by the interaction with the metal substrate, the double peak structure of the stacked dimer occurs also on gold in the appropriate spectra (1.5–2.5 ML), indicating already a quite low influence of the substrate on the second molecular layer. Hence, the second molecular layer seems to be the origin of feature *C*. The occurrence of this feature even in thicker films points to the fact that areas with larger and smaller layer thickness (2–3 ML) coexist simultaneously on the sample. Because the spectra of areas of larger layer thickness (PTCDA chain lengths in the stack $N \geqslant 4$) characterizes already almost the infinite chain, features *A* and *B* become more intense with increasing layer thickness. However, the spectral form does not change anymore. This is a nice confirmation by optically means of the finding of Fenter

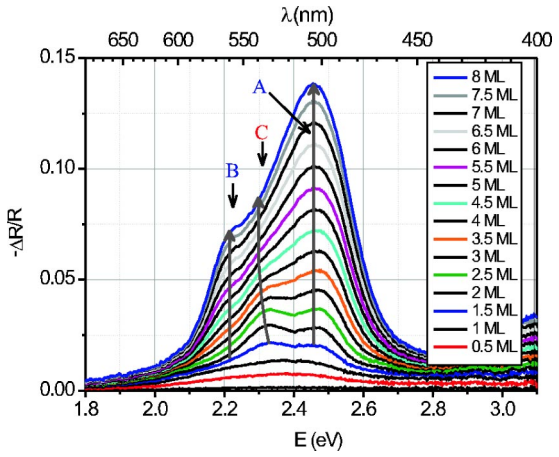

FIG. 16. (Color online) The coverage dependent differential reflectance spectra of highly ordered PTCDA on Au(111). In addition to the features *A* and *B* already present in the polycrystalline films, at 2 ML coverage a new peak *C* occurs which becomes less pronounced with further increasing film thickness.

et al.[71] of island growth (Stranski-Krastanov growth) in the case of PTCDA on Au(111). Hence, due to the superimposed spectra of different PTCDA stack lengths (i.e., film thicknesses), the shift of peak *A* is much smaller compared to *Peak1* in case of PTCDA grown on mica. For further details on this system, see Ref. 25.

V. SUMMARY AND CONCLUSIONS

We present a highly sensitive *in situ* setup for differential reflectance spectroscopy which offers unique prospects in investigating the excitonic properties of ultrathin OMCs. It is shown that the spectra obtained by this method nicely correspond to the absorption spectra in the case of films on transparent substrates like mica. In contrast, they contain a mixture of the real and imaginary part of the dielectric function of the molecular film if substrates like gold are used, which exhibit a strong dispersion in its optical constants.

In the spectra, the process of solid state formation from monomeric to oligomeric properties, and the varying influence of quantum size and on-site effects, have been manifested with increasing dimensions of the PTCDA layer. They lead to an obvious change in the spectra during the transition monomer-dimer-oligomer, and an overall spectral shift of the lowest energy absorption peak of about ~160 meV occurs. The absorption of the building blocks (the PTCDA monomers) is affected strongly by their surrounding. While the observed peak shift during the growth of the first PTCDA monolayer on mica could be attributed to both effective medium effects and screening effects, the amount of the observed shift can already exclusively be predicted by effective medium theories, which confirms the discussion in Ref. 11. Changes in the apparent oscillator strength per molecule can be explained by on-site effects. In the case of thin films of PTCDA on Au, the monomer absorption is strongly broadened due to the interaction with the substrate. Additionally, we can reason from the optical spectra that Stranski-Krastanov growth dominates, whereas in case of the substrate mica layer-by-layer growth is observed.

ACKNOWLEDGMENTS

The authors thank M. Hoffmann for helpful discussions. Financial support of this work by the "Deutsche Forschungsgemeinschaft" (DFG) via Grant No. FR 875/6, FOR 335/2 and DFG Leibnizpreis (K. Leo) is gratefully acknowledged.

*Electronic address: fritz@iapp.de

[1] S. R. Forrest, Chem. Rev. (Washington, D.C.) **97**, 1793 (1997).
[2] P. Peumans, A. Yakimov, and S. R. Forrest, J. Appl. Phys. **93**, 3693 (2003).
[3] T. Fritz, *Molecular Architecture in Heteroepitaxially Grown Organic Thin Films* (Wissenschaftlicher Fachverlag, Dresden, 1999).
[4] K. Glöckler, C. Seidel, A. Soukopp, M. Sokolowski, E. Umbach, M. Böhringer, R. Berndt, and W. Schneider, Surf. Sci. **405**, 1 (1998).
[5] S. Mannsfeld, M. Toerker, T. Schmitz-Hübsch, F. Sellam, T. Fritz, and K. Leo, Org. Electron. **2**, 121 (2001).
[6] T. Schmitz-Hübsch, F. Sellam, R. Staub, M. Törker, T. Fritz, C. Kübel, K. Müllen, and K. Leo, Surf. Sci. **445**, 358 (2000).
[7] D. Schlettwein, A. Back, B. Schilling, T. Fritz, and N. R. Armstrong, Chem. Mater. **10**, 601 (1998).
[8] E. I. Haskal, Z. Shen, P. E. Burrows, and S. R. Forrest, Phys. Rev. B **51**, 4449 (1995).
[9] Z. Shen and S. R. Forrest, Phys. Rev. B **55**, 10 578 (1997).
[10] V. M. Agranovich, R. D. Atanasov, and G. F. Bassani, Chem. Phys. Lett. **199**, 621 (1992).
[11] U. Beckers, O. Stenzel, S. Wilbrandt, U. Flake, and C. von Borczyskowski, J. Phys.: Condens. Matter **10**, 1721 (1998).
[12] M. Leonhardt, O. Mager, and H. Port, Chem. Phys. Lett. **313**, 24 (1999).
[13] V. Bulović, P. E. Burrows, S. R. Forrest, J. A. Cronin, and M. E. Thompson, Chem. Phys. **210**, 1 (1996).
[14] I. Vragović, R. Scholz, and M. Schreiber, Europhys. Lett. **57**, 288 (2002).
[15] M. Hoffmann and Z. G. Soos, Phys. Rev. B **66**, 024305 (2002).
[16] K. Schmidt, Phys. Lett. A **293**, 83 (2002).
[17] H. Proehl, T. Dienel, R. Nitsche, and T. Fritz, Phys. Rev. Lett. **93**, 097403 (2004).
[18] R. E. Hummel, Phys. Status Solidi A **76**, 11 (1983).
[19] P. Chiarada and R. Del Sole, Surf. Rev. Lett. **6**, 517 (1999).
[20] Y. Borensztein, Surf. Rev. Lett. **7**, 399 (2000).
[21] J. D. E. McIntyre and D. E. Aspnes, Surf. Sci. **24**, 417 (1971).
[22] The complex optical constant/refractive index $\hat{n}$ is associated with the (complex) dielectric function via $\hat{\epsilon}=\epsilon'-\iota\epsilon''=\hat{n}^2=(n-\iota\kappa)^2$.
[23] Scientific Computing International (SCI), FILM WIZARD® (1994–1999).
[24] M. Dignam and M. Moskovits, J. Chem. Soc., Faraday Trans. 2

69, 65 (1973).

[25] R. Nitsche, H. Proehl, and T. Fritz, in *Organic Nanophotonics*, edited by F. Charra, V. M. Agranovich, and F. Kajzar (Kluwer Academic, Dordrecht, 2003), Vol. 100 of NATO Science Series II: Mathematics, Physics and Chemistry, pp. 103–117.

[26] S. Kim, Z. Wang, and D. A. Scherson, J. Phys. Chem. B **101**, 2735 (1997).

[27] A. B. Djurišić, T. Fritz, and K. Leo, Opt. Commun. **183**, 123 (2000).

[28] According to Ref. 72, the coefficients C' and C'' can be expressed as $C'=-(8\pi/\lambda)\{\epsilon_3''/[\epsilon_3''^2+(\epsilon_3'-1)^2]\}$ and $C''=(8\pi/\lambda)\{(\epsilon_3'-1)/[\epsilon_3''^2+(\epsilon_3'-1)^2]\}$ using the substrate's dielectric function $\hat{\epsilon}_3=\epsilon_3'-\imath\epsilon_3''$.

[29] F. Sellam, T. Schmitz-Hübsch, M. Toerker, H. Proehl, K. Müllen, and K. Leo, Surf. Sci. **478**, 113 (2001).

[30] The readout time is the time it takes to shift the whole CCD rows during the read-out cycle, in our case ~25 ms.

[31] S. R. Forrest and Y. Zhang, Phys. Rev. B **49**, 11 297 (1994).

[32] M. L. Kaplan, C. S. Day, A. I. Lovinger, P. H. Schmidt, and S. R. Forrest (private communication).

[33] M. Hoffmann, K. Schmidt, T. Fritz, T. Hasche, V. M. Agranovich, and K. Leo, Chem. Phys. **258**, 73 (2000).

[34] F. Balzer and H.-G. Rubahn, Surf. Sci. **584**, 170 (2004).

[35] R. Erlandsson, G. Hadziioannou, C. M. Mate, G. M. McCelland, and S. Chiang, J. Chem. Phys. **89**, 5190 (1988).

[36] M. Odelius, M. Bernasconi, and M. Parrinello, Phys. Rev. Lett. **78**, 2855 (1997).

[37] U. Gómez, M. Leonhardt, H. Port, and H. C. Wolf, Chem. Phys. Lett. **268**, 1 (1997).

[38] M. I. Alonso, M. Garriga, N. Karl, J. O. Osso, and F. Schreiber, Org. Electron. **3**, 23 (2002).

[39] E. David, Z. Phys. **114**, 389 (1939).

[40] J. C. Maxwell-Garnett, Philos. Trans. R. Soc. London **203**, 385 (1904).

[41] D. A. G. Bruggeman, Ann. Phys. **24**, 636 (1935).

[42] G. A. Niklasson and C. G. Granquist, J. Appl. Phys. **55**, 3382 (1984).

[43] A standard LOM for $\hat{\epsilon}=\epsilon'-\imath\epsilon''$ with $\epsilon'=\epsilon_\infty'+\Sigma_j F_j^*(\omega_j^2-\omega^2)/[(\omega_j^2-\omega^2)^2+(\omega\Gamma_j)^2]$ and $\epsilon''=\Sigma_j F_j\omega_j\Gamma_j/[(\omega_j^2-\omega^2)^2+(\omega\Gamma_j)^2]$ with four transitions was used, with $\hbar\omega_j=E_j$ being the resonance frequency, F_j the strength and Γ_j the width (inverse lifetime) of the molecular excitation j. A dielectric screening of $\epsilon_\infty'>1$ would result from the influence of higher lying transitions and has to be treated energy dependent in general. However, if the next higher transitions are far away or low in intensity, ϵ_∞' can be assumed to be constant in the range of interest. The parameters used to model the monolayer were $\hbar\Gamma_j=110$ meV, $(E_j)=(2.34;2.51;2.67;2.84)$ eV, $(F_j/F_1)=(1;0.2;0.015;0.0005)$, and $\epsilon_\infty'=2$.

[44] Alternatively to the EMT of Maxwell-Garnett (Ref. 40) also other EM models for heterogeneous mixtures like the effective medium approximation of the Bruggeman type (Ref. 41) or the more general theory of Monecke (Ref. 73) can attest the observed blueshift with a decreasing amount of absorbing material, e.g., propose blueshifts between 25 meV and 40 meV for a 10% diluted PTCDA layer with respect to 100% coverage, if the DF $\hat{\epsilon}_{1\ \mathrm{ML}}$ derived above is used in the calculation.

[45] T. M. Halasinski, J. L. Weisman, R. Ruiterkamp, T. J. Lee, F. Salama, and M. Head-Gordon, J. Phys. Chem. A **107**, 3660 (2003).

[46] *IUPAC Compendium of Chemical Terminology "The Gold Book,"* 2nd ed., edited by A. D. McNaught and A. Wilkinson (Blackwell Science, New York, 1997), Vol. 66, p. 1129, www.iupac.org

[47] K. Yamamoto, M. Higuchi, S. Shiki, M. Tsuruta, and H. Chiba, Nature (London) **415**, 509 (2002).

[48] For a solid, the LOM can be considered for the atomic/molecular polarizabilities $\hat{\alpha}$. For instance, in case of an isotropic solid of particle density η, one gets from the analysis of the Clausius-Mosotti equation: $\int \mathrm{Im}(\epsilon)\omega d\omega=(\pi\eta F/2\epsilon_0)((\epsilon_\infty'+2)/3)^2$. Additionally, resonances in the solid become redshifted with respect to the isolated LOM (ω_0) via $\omega_1^2=\omega_0^2-(\eta F/3\epsilon_0)((\epsilon_\infty'+2)/3)$ (see, e.g., Chap. 2 of Ref. 74).

[49] R. Nitsche and T. Fritz, Appl. Opt. **43**, 3263 (2004).

[50] I. Vragović and R. Scholz, Phys. Rev. B **68**, 155202 (2003).

[51] I. Tonoco, Jr., J. Am. Chem. Soc. **82**, 4785 (1960).

[52] R. K. Bullough, J. Chem. Phys. **43**, 1927 (1965).

[53] J. Ferguson, J. Chem. Phys. **44**, 2677 (1966).

[54] Additionally, when analyzing the data of Bulovic *et al.* (Ref. 13) of PTCDA dissolved in NMP, we found a similar behavior the integral optical density in the concentration range of 0.434–0.867 μmol l^{-1} shows a decrease of the oscillator strength per molecule by ~50%, certainly due to the beginning aggregation of PTCDA molecules.

[55] J.-S. Lee, Opt. Eng. **25**, 636 (1986).

[56] By means of the optical constants of PTCDA (Ref. 27) and the value of the integrated absorbance for thin PTCDA films given in Ref. 15 (accuracy about ±7%), the effective thickness of the molecular layer can be evaluated. In the case of films with ⩽5 nm thickness, a value for the integral absorbance of ~2.5 cm^{-1} eV can be estimated with help of thin film simulations. Additionally, it was found that even highly ordered thin films can be described by the optical constants given in Ref. 27 (i.e., these films had a preferential orientation), so these constants were used in all further simulations.

[57] F. F. So, S. R. Forrest, Y. Q. Shi, and W. H. Steier, Appl. Phys. Lett. **56**, 674 (1990).

[58] 3,4,7,8-naphthalenetetracarboxylic dianhydride (NTCDA).

[59] Indium phthalocyanine chloride (InPc-Cl).

[60] M. L. Anderson, V. S. Williams, T. J. Schuerlein, G. E. Collins, C. D. England, L.-K. Chau, P. A. Lee, K. W. Nebesny, and N. R. Armstrong, Surf. Sci. **307-309**, 551 (1994).

[61] F. F. So and S. R. Forrest, Phys. Rev. Lett. **66**, 2649 (1991).

[62] This value of m_{eff} can be related to the exciton transfer integral J (Ref. 75). The value of $J=110$ meV would indicate a rather strong interaction, compared to recent microscopic models (Refs. 15 and 50).

[63] I. Vragović, "Fenkel exciton model of excitation and recombination processes in crystalline α-PTCDA," Ph.D. thesis, Technische Universität Chemnitz, 2003.

[64] The molecular crystals of perylene can be found in two modifications: an α modification, where the molecules are arranged in a three-dimensional herringbone manner, and a β modification where the building blocks are sandwich dimers.

[65] T. Christ, F. Petzke, P. Bordat, A. Herrmann, E. Reuther, K. Müllen, and T. Basché, J. Lumin. **98**, 23 (2002).

[66] M. H. Hennessy, Z. G. Soos, R. A. Pascal, Jr., and A. Girlando, Chem. Phys. **245**, 199 (1999).

[67] M. H. Hennessy, R. A. Pascal, Jr., and Z. G. Soos, Mol. Cryst. Liq. Cryst. Sci. Technol., Sect. A **355**, 41 (2001).

[68] Due to the fact that the absorption of a thick PTCDA layer is described, Beer's law can be applied.

[69] P. I. Cohen, G. S. Petrich, P. R. Pukite, and G. J. Whaley, Surf. Sci. **216**, 222 (1989).
[70] T. Schmitz-Hübsch, T. Fritz, F. Sellam, R. Staub, and K. Leo, Phys. Rev. B **55**, 7972 (1997).
[71] P. Fenter, F. Schreiber, L. Zhou, P. Eisenberger, and S. R. Forrest, Phys. Rev. B **56**, 3046 (1997).
[72] S. Selci, G. Chiarotti, P. Chiarada, and A. Cricenti, J. Vac. Sci. Technol. A **5**, 327 (1987).
[73] J. Monecke, J. Phys.: Condens. Matter **6**, 907 (1994).
[74] V. M. Agranovich and M. D. Galanin, *Electronic Excitation Energy Transfer in Condensed Matter*, Vol. 3 in Modern Problems in Condensed Matter Sciences (North-Holland, Amsterdam, 1982).
[75] M. Hoffmann, in *Electronic Excitations in Organic Based Nanostructures*, edited by V. Agranovich and G. Bassani, Thin Films and Nanostructures, Vol. 31 (Elsevier, New York, 2003), Chap. 5, pp. 221–292.